Journal of
Marine Science and Engineering

MDPI

Article

Power Tracking Control of Marine Boiler-Turbine System Based on Fractional Order Model Predictive Control Algorithm

Shiquan Zhao [1], Sizhe Wang [1], Ricardo Cajo [2], Weijie Ren [1,3] and Bing Li [1,*]

[1] College of Intelligent Systems Science and Engineering, Harbin Engineering University, Harbin 150001, China
[2] Facultad de Ingeniería en Electricidad y Computación, Escuela Superior Politécnica del Litoral, ESPOL, Campus Gustavo Galindo Km 30.5 Vía Perimetral, P.O. Box 09-01-5863, Guayaquil 090150, Ecuador
[3] Faculty of Electronic Information and Electrical Engineering, Dalian University of Technology, Dalian 116024, China
* Correspondence: libing265@hrbeu.edu.cn

Abstract: The marine boiler-turbine system is the core part for the steam-powered ships with complicated dynamics. To improve the power tracking performance and fulfill the requirement of high utilization rate of fossil energy, the control performance of the system should be improved. In this paper, a nonlinear model predictive control method is proposed for the boiler-turbine system with fractional order cost functions. Firstly, a nonlinear model of the boiler-turbine system is introduced. Secondly, a nonlinear extended predictive self adaptive control(EPSAC) method is designed to the system. Then, integer order cost function is replaced with a fractional order cost function to improve the control performance, and also the configuration of the cost function is simplified. Finally, the superiority of the proposed method is proved according to the comparison experiments between the fractional order model predictive control and the traditional model predictive control.

Keywords: boiler-turbine; nonlinear model predictive control; fractional order calculus; distributed control

check for updates

Citation: Zha, S.; Wang, S.; Cajo, R.; Ren, W.; Li, B. Power Tracking Control of Marine Boiler-Turbine System Based on Fractional Order Model Predictive Control Algorithm. *J. Mar. Sci. Eng.* **2022**, *10*, 1307. https://doi.org/10.3390/jmse10091307

Academic Editors: Bowen Xing, Marco Altosole, Maria Acanfora and Flavio Balsamo

Received: 7 August 2022
Accepted: 12 September 2022
Published: 15 September 2022

1. Introduction

In order to reduce the waste of fossil energy and CO_2 emissions, many countries have released different policies. China has released a policy document to fulfill its target of reaching peak carbon emissions by 2030. The United States of America released policy to cut carbon emissions in half by 2030. A lot of renewable power technologies were also proposed. However, most applied energy still comes from the combustion of fossil fuels. In addition, the control performance has a close relationship with the utilization of fossil fuels [1]. In this paper, the fossil fuels in ships are focused. Many of the ships are equipped with internal combustion engine, or gas turbine. However, for large scale ships, the power systems based on boiler-turbine still occupy a large proportion [2–4]. For example, many aircraft carriers are powered with boiler-turbine system. Hence, a lot of academics and companies are doing research to improve the control performce of the boiler-turbine system [5–9], of which there are three manipulated variables and three controlled variables with complicated dynamics. For the marine steam power plant, the disturbance and the energy required changes more frequently compared than that on land. However, there is not so much research about the control for the marine boiler-turbine system.

In the boiler-turbine system, the interactions of rvariables and constraints are the mainly reasons which make it difficult to obtain a satisfied control performance. The input variables for the system are the flow rates of fuel, steam to the turbine, and feedwater to the boiler, while the output variables are the steam pressure in the drum of the boiler, power required of the turbine, and the water level of the drum. The constraints are the limitations for the actuator, including the upper and lower bound, and rate limiter. In addition, power requirement changes a lot, which is usually treated as disturbance. In order to compensate unknown disturbances in the boiler-turbine system, a high order sliding mode observer was designed for a baseline exponentially stable feedback controller [9]. To improve the economy of the boiler-turbine system, the economic index was utilized directly in the cost function, and a global economic optimum routine was obtained for the system [10]. In the literature [11], the model of the boiler-turbine system was linearized and decoupled with an adaptive feedback linearization method, and a second order sliding mode controller was designed to deal with the disturbances and uncertainties. Ref. [12] applied an online policy iteration integral reinforcement learning method to the boiler-turbine system, and optimal tracking control performance was obtained.

The model predictive control(MPC) has the advantages in dealing with the nonlinear dynamics, interactions and constraints problems [13], hence, MPC is a preferred choice for researchers. The MPC is studied in many fields such as building energy management [14], landscape office lighting regulatory system [15,16], wind turbines [17], tank-system [18], pressure oscillation adsorption process [19,20], permanent-magnet synchronous motor [21], autonomous underwater vehicle [22], and so on. For the boiler-turbine system, there are also some applications of MPC. A nonlinear model predictive control method was designed for boiler-turbine system with a data driven model [23], and the optimal problem was solved by immune genetic algorithm. Ref. [24] presented a zone economic model predictive cotroller to fulfill the economic target of the boiler-turbine system. Fuzzy model predictive control was designed to realize load tracking and economy of the boiler-turbine system, and a fuzzy model was used to approximate the nonlinear dynamics of the system [25]. Other MPC applications on boiler-turbine system can be found in [26–28].

For the MPC method, the weighting factors have a significant different effect on the control performance, and the number of the weighting factors is large, which makes it diffcult to obtain a good choice for these parameters. For example, if the N_{ip} denotes the prediction horizon for the ith output, and N_{jc} for the jth control horizon, the number of weighting factor will be $\sum_{i=1}^{n} N_{ip} + \sum_{j=1}^{m} N_{jc}$, where m and n are the numbers of output and input. The commonly used method to tune the weighting factors is trial and error or choose them empirically. Another alternative way to choose the control parameters is optimization method [29,30]. However, due to the high dimension of the weighting factors, it is difficult to optimize them. So, in this paper, the fractional order model predictive control(FOMPC) for the boiler-turbine system is proposed. By two fractional order papermeters (one for the tracking error, and another for the control effort), the weight factors matrices can be obtained, which reduces the difficulties in weighting factors configuration. The boiler-turbine system is a nonlinear multiple inputs and multiple outputs system, so the nonlinear distributed structure of MPC is studied for the system.

The rest of the paper is structured as follows. The boiler-turbine system is formulated in Section 2; Section 3 presents the nonlinear distributed MPC with EPSAC framework. Fractional order MPC is designed for the boiler-turbine system in the Section 4. The simulation experiments are presented in Section 5. The last section gives the conclusions.

2. Boiler-Turbine System

The boiler-turbine system is a core part in the power plant, and Figure 1 shows the structure of the system [9]. The details elements are indicated in the figure, and they are listed as follows: 1—drum; 2—superheater; 3—water spray desuperheater; 4—valve for the steam to turbine; 5—turbine high-pressure cylinders; 6—foward control valve; 7—backward control valve; 8—turbine middle- and low- pressure cylinders; 9—shafting; 10—condenser; 11—replenish water; 12—condensate pump; 13—low-pressure heater; 14—deaerator; 15—feed water pump; 16—high-pressure heater; 17—feed water valve; 18—economizer; 19—downcomers; 20—water-cooled walls; 21—furnace; 22—heat flow control valve; 23—nozzle; 24—blower; 25—preheater for air; 26—air conditioner; 27—flue gas baffle; 28—induced draft fan; 29—flue; 30—gearbox; 31—turbine.

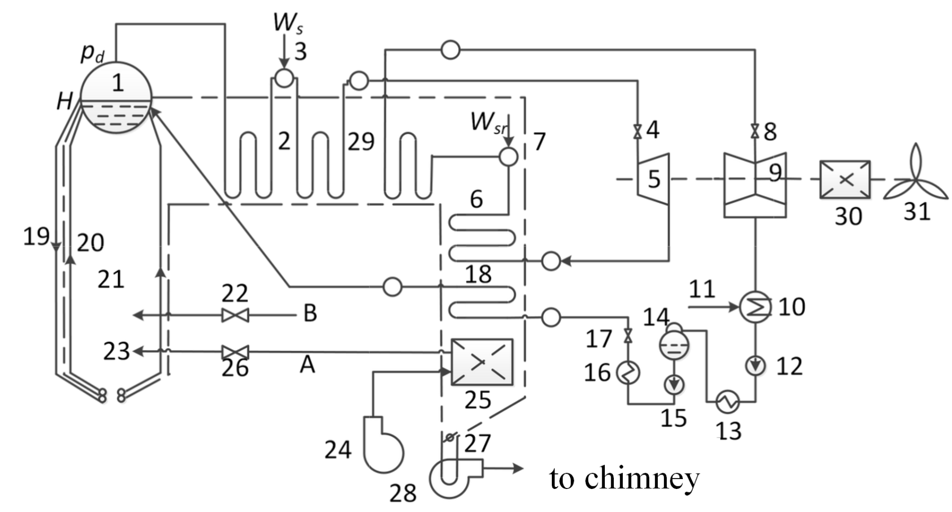

Figure 1. The structure of a boiler-turbine unit.

Due to the lack of data for marine boiler-turbine sytem, it is difficult to obtain its model. The structure is similar to that on land. Hence, a model of on load power plant is chosen for study, and the nonlinear model of the boiler-turbine system is shown as follows according to the literature [31]:

$$\dot{x}(t) = F(x(t)) + G(x(t))u(t), \tag{1}$$

and the $F(x(t))$, $G(x(t))$ are defined as follows:

$$F(x(t)) = \begin{bmatrix} 0 \\ -0.1x_2 - 0.016x_1^{9/8} \\ 0.0022x_1 \end{bmatrix} \tag{2}$$

$$G(x(t)) = \begin{bmatrix} 0.9 & -0.0018x_1^{9/8} & -0.15 \\ 0 & 0.073x_1^{9/8} & 0 \\ 0 & -0.0129x_1 & 1.6588 \end{bmatrix} \tag{3}$$

where the inputs $u = [u_1, u_2, u_3]^T$ for the system are the valve opening of fuel, steam to the turbine and feedwater to the drum. The states are drum steam pressure, power required for the turbine and steam water density denoted by $x = [x_1, x_2, x_3]^T$. The outputs are drum steam pressure, power required for the turbine and water level in the drum. The level of the drum can be calculated as:

$$L = 0.05(0.13073x_3 + 100\alpha_s + q_e/9 - 67.975) \tag{4}$$

and $q_e = (0.854u_2 - 0.147)x_1 + 45.59u_1 - 2.51u_3 - 2.096$; $\alpha_s = \frac{(1-0.001538x_3)(0.8x_1-25.6)}{x_3(1.0394-0.0012304x_1)}$. The q_e and α_s denote the evaporation rate and steam quality, respectively.

The rates and amplitudes limitaion for the inputs are listed as follows:

$$\begin{cases} -0.007 \leq \frac{du_1}{dt} \leq 0.007 & 0 \leq u_1 \leq 1 \\ -2.0 \leq \frac{du_2}{dt} \leq 0.02 & 0 \leq u_2 \leq 1 \\ -0.05 \leq \frac{du_3}{dt} \leq 0.05 & 0 \leq u_3 \leq 1 \end{cases} \tag{5}$$

For the boiler-turbine, there are different operating points. To evaluate the effectiveness of the proposed method, experiments around the following operating points shown in Table 1 are carried out.

Table 1. Operating points for the boiler-turbine system.

Operating Point	Pressure	Power	Density
1	99.3 kg/m^2	80.9 MW	396
2	120 kg/m^2	110 MW	331

The drum water level should always be kept as zero meters.

3. Nonlinear Distributed MPC for the Boiler-Turbine System

According to the introduction of the boiler-turbine, it can be found that this system is a nonlinear multiple inputs multiple outputs system. Hence, the nonlinear MPC is designed for the system with distributed structure.

3.1. The Basic of the EPSAC

This part presents the basic of EPSAC. For more details about the EPSAC, it can be found in the refs. [32–34]. For a discrete system, the system output can be expressed as:

$$y(t) = x(t) + w(t) \tag{6}$$

where $y(t)$ is the system output; $x(t)$ is the model output and the $w(t)$ is the disturbances. $x(t)$ can be calculated according to the model of the system as follow:

$$x(t) = f[x(t-1), x(t-2), \ldots, u(t-1), u(t-2), \ldots] \tag{7}$$

In Equation (7), the $f(x,u)$ denotes the model of the system, $x(t-i)$ and $u(t-i)$ $i = 1, 2, \ldots$ indicate the past model outputs and inputs.

In the EPSAC, the input scenario for the future is composed with two parts:

$$u(t+k|t) = u_{base}(t+k|t) + \delta u(t+k|t) \tag{8}$$

where the $u_{base}(t+k|t)$ and $\delta u(t+k|t)$ are the basic and optimized future control actions. Then the future system output can be predicted as:

$$y(t+k|t) = y_{base}(t+k|t) + y_{opt}(t+k|t) \tag{9}$$

where $y_{base}(t+k|t)$ is the result of the basic future control action; $u_{base}(t+k|t)$ and $y_{opt}(t+k|t)$ can be calculated according to the optimized future control action $\delta u(t+k|t)$.

The $y_{opt}(t+k|t)$ can be obtained with:

$$y_{opt}(t+k|t) = h_k \delta u(t|t) + h_{k-1} \delta u(t+1|t) + \ldots + g_{k-N_c+1} \delta u(t+N_c-1|t) \tag{10}$$

In Equation (10), the h_i and g_i are the impulse response and step response coefficients of the system, respectively; N_c and N_p are the control horizon and the prediction horizon, respectively. The system output can be re-written in matrix form:

$$\mathbf{Y} = \bar{\mathbf{Y}} + \mathbf{GU} \tag{11}$$

where $\mathbf{Y} = [y(t+N_1|t) \ldots y(t+N_p|t)]^T$, $\mathbf{U} = [\delta u(t|t) \ldots \delta u(t+N_c-1|t)]^T$, $\bar{\mathbf{Y}} = [y_{base}(t+N_1|t) \ldots y_{base}(t+N_P|t)]^T$; N_1 is the time delay of the system, and

$$\mathbf{G} = \begin{bmatrix} h_{N_1} & h_{N_1-1} & \cdots & g_{N_1-N_c+1} \\ h_{N_1+1} & h_{N_1} & \cdots & \cdots \\ \cdots & \cdots & \cdots & \cdots \\ h_{N_P} & h_{N_P-1} & \cdots & g_{N_P-N_c+1} \end{bmatrix}$$

The disturbance term $w(t)$ in (6) includes all the effects on the system output. It can be modeled by a colored noise process as:

$$w(t+k|t) = \frac{C(q^{-1})}{D(q^{-1})} w_f(t+k|t) \tag{12}$$

where q^{-1} is the backward shift operator.

In this work, the $C(q^{-1})$ and $D(q^{-1})$ are designed as follows:

$$\frac{C(q^{-1})}{D(q^{-1})} = \frac{1}{(1-q^{-1})(1-ae^{+j\alpha}q^{-1})(1-ae^{-j\alpha}q^{-1})} \tag{13}$$

with $\alpha = 2\pi f_0 T_s$ and $a \approx 1$; T_s is the sampling time and $a \leq 1$ for stability.

The cost function for the boiler-turbine system can be defined as:

$$J_{MPC} = \sum_{k=N_1}^{N_2} p_k [r(t+k|t) - y(t+k|t)]^2 + \sum_{k=1}^{N_u} q_k \triangle u(t+k)^2 \tag{14}$$

The p_k and q_k are nonnegative weighting factors, and they are usually kept as constants.

The matrix form of Equation (14) can be written as:

$$J_{MPC} = (\mathbf{R}-\mathbf{Y})^T \mathbf{P} (\mathbf{R}-\mathbf{Y}) + \mathbf{U}^T \mathbf{Q} \mathbf{U} = (\mathbf{R}-\bar{\mathbf{Y}}-\mathbf{G}\mathbf{U})^T \mathbf{P} (\mathbf{R}-\bar{\mathbf{Y}}-\mathbf{G}\mathbf{U}) + \mathbf{U}^T \mathbf{Q} \mathbf{U} \tag{15}$$

with $P = diag(p_1, p_2, \ldots, p_{(N_2-N_1+1)})$ and $Q = diag(q_1, q_2, \ldots, q_{N_u})$.

For systems with constraint, the optimization problem can be solved with quadratic programming. Otherwise, the results of the optimal input part, which are indicated by $\delta u(t+k|t)$, can be obtained as:

$$\mathbf{U}^*_{\mathbf{MPC}} = (\mathbf{G}^T \mathbf{P} \mathbf{G} + \mathbf{Q})^{-1} \mathbf{G}^T \mathbf{P} (\mathbf{R} - \bar{\mathbf{Y}}) \tag{16}$$

3.2. The Fractional Order MPC

For the fractional order MPC, the cost function is designed as:

$$J_{FOMPC} = {}^{\gamma} I_{N_1}^{N_2} p_k [r(t+k|t) - y(t+k|t)]^2 + {}^{\lambda} I_1^{N_c} q_k \triangle u(t+k)^2 \tag{17}$$

where ${}^{\gamma}I_{N_1}^{N_2}$ and ${}^{\lambda}I_1^{N_c}$ indicate fractional order integral with fraction order of γ and λ; [N_1, N_2] and [1, N_c] are the integration intervals.

According to [35], the Equation (17) can be written by:

$$\begin{aligned} J_{FOMPC} &= (\mathbf{R}-\mathbf{Y})^T \mathbf{P} \mathbf{\Gamma}(T_s,\gamma)(\mathbf{R}-\mathbf{Y}) + \mathbf{U}^T \mathbf{Q} \mathbf{\Lambda}(T_s,\lambda) \mathbf{U} \\ &= (\mathbf{R}-\bar{\mathbf{Y}}-\mathbf{G}\mathbf{U})^T \mathbf{P} \mathbf{\Gamma}(T_s,\gamma)(\mathbf{R}-\bar{\mathbf{Y}}-\mathbf{G}\mathbf{U}) + \mathbf{U}^T \mathbf{Q} \mathbf{\Lambda}(T_s,\lambda) \mathbf{U} \end{aligned} \tag{18}$$

$$\mathbf{\Gamma}(T_s,\gamma) = T_s^{\gamma} diag(m_{N_2-N_1}, m_{N_2-N_1-1}, \ldots, m_1, m_0) \tag{19}$$

$$\mathbf{\Lambda}(T_s,\lambda) = T_s^{\lambda} diag(m_{N_c}, m_{N_c-1}, \ldots, m_1, m_0) \tag{20}$$

The m_i in Equations (19) and (20) with fractional order α can be calculated as:

$$m_j = \omega_j^{(-\alpha)} - \omega_{j-n}^{(-\alpha)} \tag{21}$$

where n is the number of the m_i, and ω can be calculated with:

$$\omega_j^{-\alpha} = \begin{cases} (1-(1-\alpha)/j)\omega_{j-1}^{(-\alpha)} & j > 0; \\ 1 & j = 0; \\ 0 & j < 0. \end{cases} \tag{22}$$

According to Equation (19) to Equation (22), the weight matrix in the cost function J_{FOMPC} can be easily tuned with fractional order γ and λ. For system with constraints, the optimization for input sequence can be solved with quadratic programming. For the case without constraints, the results for the optimal input $\delta u(t+k|t)$ can be calculated as:

$$\mathbf{U}^{*}_{\mathbf{FOMPC}} = (\mathbf{G}^{T}\mathbf{P}(\boldsymbol{\Gamma}+\boldsymbol{\Gamma}^{\mathbf{T}})\mathbf{G}+\mathbf{Q}(\boldsymbol{\Lambda}+\boldsymbol{\Lambda}^{\mathbf{T}}))^{-1}\mathbf{G}^{T}\mathbf{P}(\boldsymbol{\Gamma}+\boldsymbol{\Gamma}^{\mathbf{T}})(\mathbf{R}-\bar{\mathbf{Y}}) \quad (23)$$

3.3. Application of the Fractional Order EPSAC to the Nonlinear MIMO System with Distributed Structure

The fractional order MPC introduced above is for the linear case. In order to apply the FOMPC to the boiler-turbine system, the nonlinear FOMPC is studied. According to the Equation (8) and (9), the principle of superposition is applied for linear system. To get over the superposition, the optimal future input $\delta u(t+k|t)$ should be removed iteratively smaller tends to zero [36]. The procedure for the nonlinear MPC is summarized as follows:

- Choose an initial base input sequence $u_{base}(t+k|t), k = 0 \dots N_u - 1$, this part should be as close as possible to the optimal input $u(t+k|t)$ to make the $\delta u(t+k|t)$ close to zero, which means that the term $y_{opt}(t+k|t)$ equals to zero;
- After chooseing the base future input, the $\delta u(t+k|t)$ can be calculated. The $\delta u(t+k|t)$ is not close to zero at the moment;
- Take the $u(t+k|t)$ from the second step as the new $u_{base}(t+k|t)$, and calculate $\delta u(t+k|t)$ again.
- Repeat step 2 and 3 until the $\delta u(t+k|t)$ is as close as possible to zero, then the $u_{base}(t+k|t)$ can be applied to the system at the time $t+1$.

The flow chart of nonlinear MPC is shown in Figure 2.

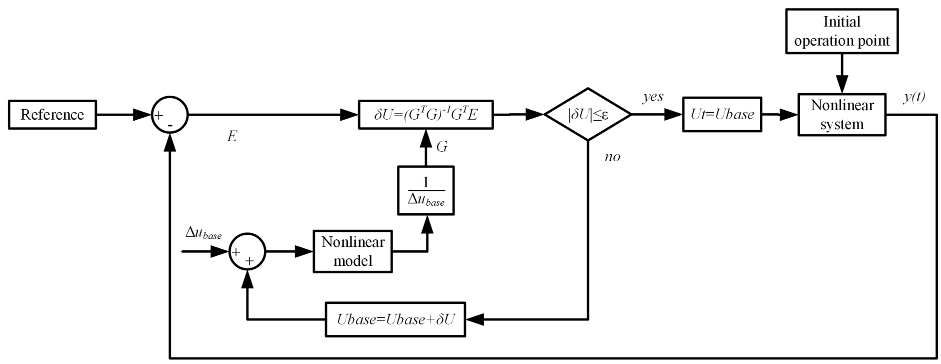

Figure 2. The flow chart of nonlinear MPC.

The boiler-turbine is a MIMO system, and there are strong interactions between variables. In order to calculate the optimal input sequence, the effect from coupling variables should be considered and the communication network should be established. In this work, the distributed structure is applied. The pseudocode is provided in Algorithm 1.

The boiler-turbine system is a nonlinear MIMO system, hence, the nonlinear MPC with distributed scheme will be applied. According to the procedure of nonlinear MPC and algorithm for the distributed MPC, the optimal future input sequence should fulfill the follow conditions:

$$\begin{cases} |||\delta \mathbf{U}_i^{iter+1} - \delta \mathbf{U}_i^{iter}|| \leqslant \varepsilon_i) \\ \delta \mathbf{U}_i^{iter+1} \approx 0. \end{cases} \quad (24)$$

Algorithm 1 Algorithm for the distributed MPC

1: The loop i receives an optimal local control action $\delta\mathbf{U}_i$ for the first time, which will be marked as $iter = 0$, and the local control action $\delta\mathbf{U}_i$ can be marked as $\delta\mathbf{U}_i^{iter}$, where $\delta\mathbf{U}_i$ indicates the vector of the optimizing future control actions with length of N_{ci};

2: The information of coupling variables $\delta\mathbf{U}_j^{iter}$ ($j \in N_i$, $N_i = \{j \in N : \mathbf{G}_{ij} \neq 0\}$) will be sent to the loop i, and the $\delta\mathbf{U}_i^{iter+1}$ will be recalculated with the information of $\delta\mathbf{U}_j^{iter}$ from other loops;

3: The termination condition can be designed as: $(||\delta\mathbf{U}_i^{iter+1} - \delta\mathbf{U}_i^{iter}|| \leqslant \varepsilon_i) \vee (iter + 1 > \overline{iter})$. where ε is a positive constant and $\overline{iter}$ indicates the upper bound of the number of iteration times. If the termination condition is reached, the $\delta\mathbf{U}_i^{iter+1}$ will be adopted to the system. Otherwise, $iter = iter + 1$, and return to the Step 2.

4: The final optimal control effort can be obtained as $\mathbf{U}_t = \mathbf{U}_{base} + \delta\mathbf{U}^{iter}$, which will be applied to the system;

5: $t = t + 1$, return to Step 1.

4. Simulation of the Fractional Order MPC on Boiler-Turbine System

This section shows the simulation results of the fractional order MPC. Firstly, different fractional order terms are applied to different loops. Then, the best fractional order terms are applied to the drum steam pressure loop, power for turbine loop and water level loop, and the results are compared with the integer order MPC. Finally, the results are discussed.

The parameters configuration are listed in Table 2.

Table 2. Parameters for the MPC.

Parameters	N_c	T_s	N_p	N_1	N_s
Values	$N_{c1} = 1$, $N_{c2} = 1$, $N_{c3} = 1$ samples	5s	$N_{p1} = 15$, $N_{p2} = 15$, $N_{p3} = 15$ samples	1	100

In Table 2, N_{ci} and N_{pi} ($i = 1, 2, 3$) are control horizon and prediction horizon, respectively; N_s is the number of simulation steps. The termination conditions for the nonlinear iteration are set as: $\delta\mathbf{U}_i^{iter} \leqslant 0.05$; or the iteration times $iter_{nmpc} > 5$. The termination conditions for the distributed MPC are set as: $||\delta\mathbf{U}_i^{iter+1} - \delta\mathbf{U}_i^{iter}|| \leqslant 0.005$; or $iter > 5$.

4.1. The Influence of Fractional Order Terms to the Different Loops

In order to test the effect of different fractional order on the control performance, different fractional order terms are introduced to the cost function for each loop. The details for fractional order terms are listed in Table 3. In this work, the γ for the reference tracking and λ for the control effort are chosen the same for simplification.

Table 3. Fractional order terms for each loop.

Loops	**Fractional Order Terms**
Drum steam pressure loop	[0.5, 1, 1.5, 3]
Power loop	[0.8, 1, 1.2, 1.5]
Drum water level loop	[0.5, 1, 1.7, 2, 2.5]

According to the results shown in Figures 3–5, it can be seen that the effectiveness of different fractional order terms varies a lot. For the drum steam pressure control, the best fractional order term is 1.5; for the required power control, it is 1; and for the drum water level control, the fractional order term of 1.7 is the best.

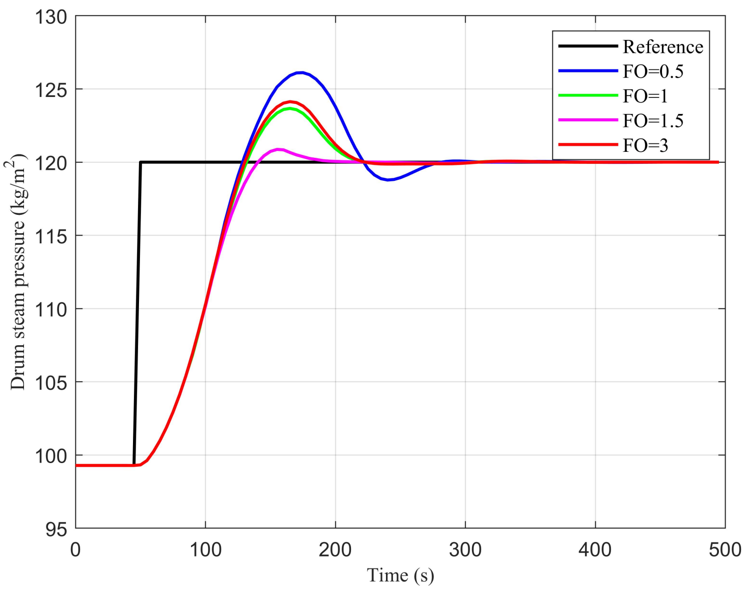

Figure 3. The drum steam pressure with different fractional orders.

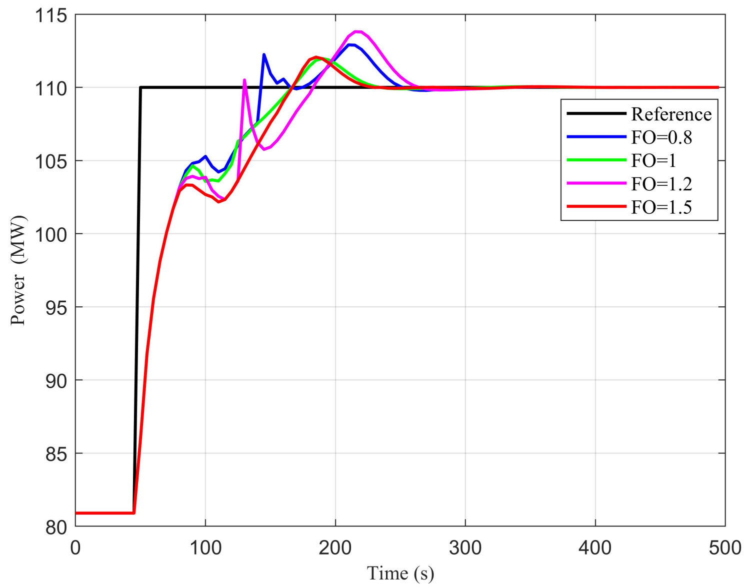

Figure 4. The required power for turbine with different fractional orders.

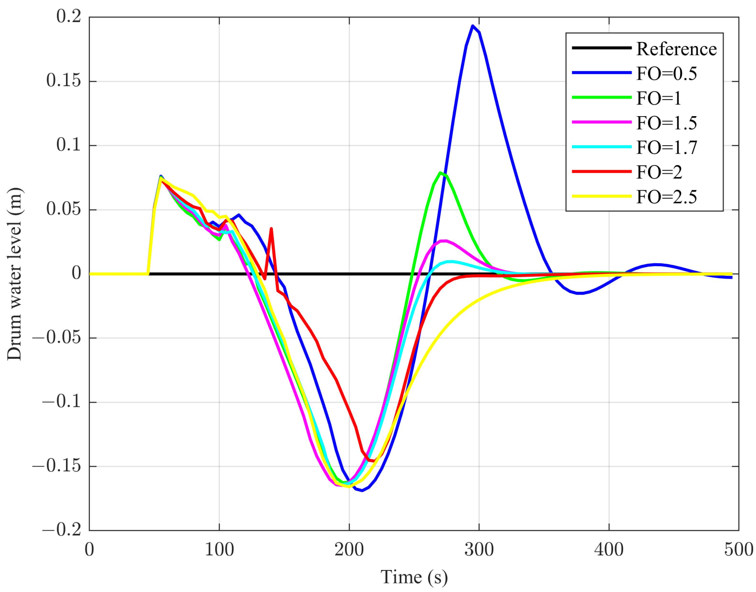

Figure 5. The drum water level with different fractional orders.

4.2. The Influence of Fractional Order Terms to the Different Loops

This section shows the comparison experiment between FOMPC and traditional MPC. The fractional order terms applied in the boiler-turbine system are chosen as 1.5, 1, 1.7 for the three loops, respectively.

In order to evaluate the effectiveness of the proposed method, the following performance indexes are compared, including Integrated Absolute Relative Error ($IARE$), Integral Secondary control output (ISU), Ratio of Integrated Absolute Relative Error ($RIARE$), Ratio of Integral Secondary control output ($RISU$) and combined index (J).

$$IARE_i = \sum_{k=0}^{N_s-1} |r_i(k) - y_i(k)|/r_i(k) \quad (i = 1,2,3) \tag{25}$$

$$ISU_i = \sum_{k=0}^{N_s-1} (u_i(k) - u_{ssi}(k))^2 \quad (i = 1,2,3) \tag{26}$$

$$RIARE_i(C_2, C_1) = \frac{IARE_i(C_2)}{IARE_i(C_1)} \quad (i = 1,2,3) \tag{27}$$

$$RISU_i(C_2, C_1) = \frac{ISU_i(C_2)}{ISU_i(C_1)} \quad (i = 1,2,3) \tag{28}$$

$$J(C_2, C_1) = \frac{1}{3} \sum_{i=1}^{3} \frac{w_1 RIARE_i(C_2, C_1) + w_2 RISU_i(C_2, C_1)}{w_1 + w_2} \tag{29}$$

where u_{ssi} is the steady state value of ith input; C_1,C_2 are the two compared controllers; the weighting factors w_1 and w_2 in equation (29) are chosen as $w_1 = w_2 = 0.5$.

The combined index J for the reference tracking case is 0.6564. From Figure 6, Tables 4 and 5, it shows that the IARE and ISU of fractional order MPC are both smaller than that of traditional MPC, which means the fractional order MPC can obtain better performance with less control effort changes. By choosing suitable fractional order terms, the fractional order MPC shows superiority compared with integer order MPC.

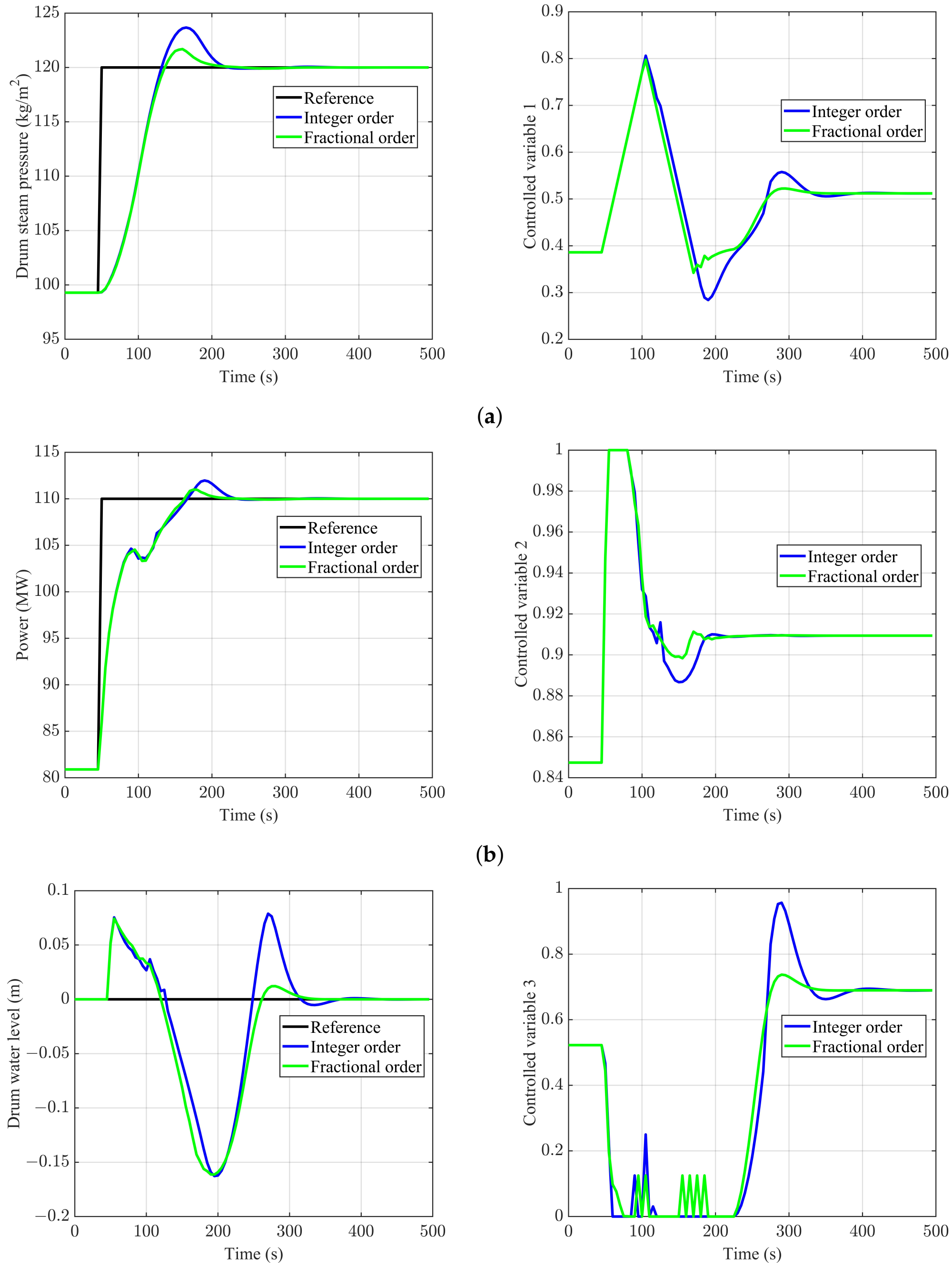

(**a**)

(**b**)

(**c**)

Figure 6. Outputs and inputs of the boiler-turbine system with FOMPC and MPC in the reference tracking experiment (the outputs are listed on the left hand, and the inputs are listed on the right hand). (**a**) control loop for drum steam pressure, (**b**) control loop for required power, (**c**) control loop for drum water level.

Table 4. Performance indexes for $IARE$ and ISU in the power reference tracking experiment.

Index		Drum Steam Pressure	Power	Drum Water Level
$IARE$	MPC	2.0072	1.5837	3.5389
	FOMPC	1.8342	1.4955	3.4534
ISU	MPC	1.1961	0.1068	18.8118
	FOMPC	0.9444	0.1042	17.1870

Table 5. Performance indexes for $RIARE$ and $RISU$ in the power reference tracking experiment (MPC is the C_2 and FOMPC the C_1 according to Equations (27) and (28)).

Index	Drum Steam Pressure	Power	Drum Water Level
$RIARE$	1.0943	1.0590	1.0248
$RISU$	1.2664	1.0251	1.0945

5. Conclusions

This paper proposed a fractional order model predictive controller for the boiler-turbine system. Due to the nonlinearity and multiple variables of the boiler-turbine, the nonlinear MPC with distributed scheme is designed, and the termination conditions are given. The integer order cost function is replaced with the fractional order cost function, which simplified the configration of the weighting factor matrices in the cost function. The number of weighting factors required to be tuned decreases from $N_p + N_c$ to two. According to the simulation for power tracking, it is proved that the fractional order MPC improves the control performance compared with the traditional MPC method. In this work, better control performance is obtained with fractional order MPC; however, how the fractional order effects the control performance is not clear, which can be researched further in the future.

Author Contributions: Methodology, S.Z.; software, S.W.; validation, S.W., R.C. and W.R.; formal analysis, S.W., R.C. and B.L.; writing—original draft preparation, S.Z.; writing—review and editing, S.Z., S.W., R.C., W.R. and B.L.; supervision, S.Z.; project administration, S.Z. and B.L.; funding acquisition, S.Z. and B.L. All authors have read and agreed to the published version of the manuscript.

Funding: This research was funded by Natural Science Foundation of Heilongjiang under grant KY10400210217, Foundation of Fundamental Strengthening Program for Technical Field under grant 2021-JCJQ-JJ-0026, Fundamental Research Funds for the Central Universities undergrant 3072020CFT1501 and Foundation of High-level scientific research guidance project of Harbin Engineering University under grant 3072022QBZ0406.

Institutional Review Board Statement: Not applicable.

Informed Consent Statement: Not applicable.

Data Availability Statement: Not applicable.

Conflicts of Interest: The authors declare no conflict of interest.

References

1. Yang, F.; Tang, C.; Antonietti, M. Natural and artificial humic substances to manage minerals, ions, water, and soil microorganisms. *Chem. Soc. Rev.* **2021**, *50*, 6221–6239. [CrossRef] [PubMed]
2. Zeńczak, W.; Gromadzińska, A.K. Preliminary Analysis of the Use of Solid Biofuels in a Ship's Power System. *Pol. Marit. Res.* **2020**, *27*, 67–79. [CrossRef]
3. Başhan, V.; Demirel, H. Application of Fuzzy Dematel Technique to Assess Most Common Critical Operational Faults of Marine Boilers. *Politek. Derg.* **2019**, *22*, 545–555. [CrossRef]
4. Luschtinetz, T.; Zeńczak, W.; Łuszczyński, D. The Selected Results of the Experimental Research of Solid Fuel Pneumatic Transportation to Ship's Boiler. *Manag. Syst. Prod. Eng.* **2019**, *27*, 144–148. [CrossRef]

5. Taler, J.; Zima, W.; Ocłoń, P.; Grądziel, S.; Taler, D.; Cebula, A.; Jaremkiewicz, M.; Korzeń, A.; Cisek, P.; Kaczmarski, K.; et al. Mathematical model of a supercritical power boiler for simulating rapid changes in boiler thermal loading. *Energy* **2019**, *175*, 580–592. [CrossRef]
6. Lu, X.; Liu, Z.; Ma, L.; Wang, L.; Zhou, K.; Feng, N. A robust optimization approach for optimal load dispatch of community energy hub. *Appl. Energy* **2020**, *259*, 114195. [CrossRef]
7. Piraisoodi, T.; Iruthayarajan, M.W.; Kadhar, K.M.A. An Optimized Nonlinear Controller Design for Boiler–Turbine System Using Evolutionary Algorithms. *IETE J. Res.* **2018**, *64*, 451–462. [CrossRef]
8. Wang, D.; Zhou, Y.; Li, X. A dynamic model used for controller design for fast cut back of coal-fired boiler-turbine plant. *Energy* **2018**, *144*, 526–534. [CrossRef]
9. Su, Z.g.; Zhao, G.; Yang, J.; Li, Y.g. Disturbance Rejection of Nonlinear Boiler–Turbine Unit Using High-Order Sliding Mode Observer. *IEEE Trans. Syst. Man Cybern. Syst.* **2018**, *50*, 5432–5443. [CrossRef]
10. Liu, X.; Cui, J. Economic model predictive control of boiler-turbine system. *J. Process. Control.* **2018**, *66*, 59–67. [CrossRef]
11. Tian, Z.; Yuan, J.; Xu, L.; Zhang, X.; Wang, J. Model-based adaptive sliding mode control of the subcritical boiler-turbine system with uncertainties. *ISA Trans.* **2018**, *79*, 161–171. [CrossRef] [PubMed]
12. Wei, Q.; Liu, Y.; Lu, J.; Ling, J.; Luan, Z.; Chen, M. A New Integral Critic Learning for Optimal Tracking Control with Applications to Boiler-Turbine Systems. *Optim. Control Appl. Methods* **2021**. [CrossRef]
13. Köhler, J.; Soloperto, R.; Müller, M.A.; Allgöwer, F. A computationally efficient robust model predictive control framework for uncertain nonlinear systems. *IEEE Trans. Autom. Control* **2020**, *66*, 794–801. [CrossRef]
14. Reynolds, J.; Rezgui, Y.; Kwan, A.; Piriou, S. A zone-level, building energy optimisation combining an artificial neural network, a genetic algorithm, and model predictive control. *Energy* **2018**, *151*, 729–739. [CrossRef]
15. Chi, C.; Cajo, R.; Zhao, S.; Liu, G.P.; Ionescu, C.M. Fractional Order Distributed Model Predictive Control of Fast and Strong Interacting Systems. *Fractal Fract.* **2022**, *6*, 179. [CrossRef]
16. Ghita, M.; Cajo Diaz, R.A.; Birs, I.R.; Copot, D.; Ionescu, C.M. Ergonomic and economic office light level control. *Energies* **2022**, *15*, 734. [CrossRef]
17. Song, D.; Chang, Q.; Zheng, S.; Yang, S.; Yang, J.; Joo, Y.H. Adaptive model predictive control for yaw system of variable-speed wind turbines. *J. Mod. Power Syst. Clean Energy* **2020**, *9*, 219–224. [CrossRef]
18. Sorcia-Vázquez, F.; Garcia-Beltran, C.; Valencia-Palomo, G.; Brizuela-Mendoza, J.; Rumbo-Morales, J. Decentralized robust tube-based model predictive control: Application to a four-tank-system. *Rev. Mex. Ingeniería Química* **2020**, *19*, 1135–1151. [CrossRef]
19. Rumbo Morales, J.Y.; López López, G.; Alvarado, V.M.; Torres Cantero, C.A.; Azcaray Rivera, H.R. Optimal Predictive Control for a Pressure Oscillation Adsorption Process for Producing Bioethanol. *Comput. Sist.* **2019**, *23*, 1593–1617.
20. Morales, J.Y.R.; López, G.L.; Martínez, V.M.A.; Vázquez, F.d.J.S.; Mendoza, J.A.B.; García, M.M. Parametric study and control of a pressure swing adsorption process to separate the water-ethanol mixture under disturbances. *Sep. Purif. Technol.* **2020**, *236*, 116214. [CrossRef]
21. Zhang, X.; Zhang, L.; Zhang, Y. Model predictive current control for PMSM drives with parameter robustness improvement. *IEEE Trans. Power Electron.* **2018**, *34*, 1645–1657. [CrossRef]
22. Shen, C.; Shi, Y.; Buckham, B. Trajectory tracking control of an autonomous underwater vehicle using Lyapunov-based model predictive control. *IEEE Trans. Ind. Electron.* **2017**, *65*, 5796–5805. [CrossRef]
23. Zhu, H.; Zhao, G.; Sun, L.; Lee, K.Y. Nonlinear predictive control for a boiler–turbine unit based on a local model network and immune genetic algorithm. *Sustainability* **2019**, *11*, 5102. [CrossRef]
24. Zhang, Y.; Decardi-Nelson, B.; Liu, J.; Shen, J.; Liu, J. Zone economic model predictive control of a coal-fired boiler-turbine generating system. *Chem. Eng. Res. Des.* **2020**, *153*, 246–256. [CrossRef]
25. Liu, X.; Cui, J. Fuzzy economic model predictive control for thermal power plant. *IET Control Theory Appl.* **2019**, *13*, 1113–1120. [CrossRef]
26. Wang, G.; Wu, J.; Ma, X. A nonlinear state-feedback state-feedforward tracking control strategy for a boiler-turbine unit. *Asian J. Control* **2020**, *22*, 2004–2016. [CrossRef]
27. Kong, L.; Yuan, J. Disturbance-observer-based fuzzy model predictive control for nonlinear processes with disturbances and input constraints. *ISA Trans.* **2019**, *90*, 74–88. [CrossRef]
28. Cui, J.; Chai, T.; Liu, X. Deep-neural-network-based economic model predictive control for ultrasupercritical power plant. *IEEE Trans. Ind. Inform.* **2020**, *16*, 5905–5913. [CrossRef]
29. Sanchez, R.O.; Rumbo Morales, J.Y.; Ortiz Torres, G.; Pérez Vidal, A.F.; Valdez Resendiz, J.E.; Sorcia Vázquez, F.d.J.; Nava, N.V. Discrete State-Feedback Control Design with D-Stability and Genetic Algorithm for LED Driver Using a Buck Converter. *Int. Trans. Electr. Energy Syst.* **2022**, *2022*, 8165149. [CrossRef]
30. Nedić, A.; Liu, J. Distributed optimization for control. *Annu. Rev. Control Robot. Auton. Syst.* **2018**, *1*, 77–103. [CrossRef]
31. Bell, R.; Åström, K.J. *Dynamic Models for Boiler-Turbine-Alternator Units: Data Logs and Parameter Estimation for a 160 MW Unit*; Technical Reports; Lund Institute of Technology: Lund, Sweden, 1987; TRFT-3192.
32. De Keyser, R. Model based predictive control for linear systems. In *UNESCO Encyclopaedia of Life Support Systems, Robotics and Automation*; Article Contribution 6.43.16.1; Eolss Publishers Co., Ltd.: Oxford, UK, 2003; Volume XI.

33. De Keyser, R.; Ionescu, C.M. The disturbance model in model based predictive control. In Proceedings of the Proceedings of 2003 IEEE Conference on Control Applications, Istanbul, Turkey, 25 June 2003; IEEE: Piscataway, NJ, USA, 2003; Volume 1, pp. 446–451.
34. Fernandez, E.; Ipanaque, W.; Cajo, R.; De Keyser, R. Classical and advanced control methods applied to an anaerobic digestion reactor model. In Proceedings of the 2019 IEEE CHILEAN Conference on Electrical, Electronics Engineering, Information and Communication Technologies (CHILECON), Valparaiso, Chile, 13–27 November 2019; IEEE: Piscataway, NJ, USA, 2019; pp. 1–7.
35. Romero, M.; de Madrid, A.P.; Vinagre, B.M. Arbitrary real-order cost functions for signals and systems. *Signal Process.* **2011**, *91*, 372–378. [CrossRef]
36. Zhao, S.; Cajo, R.; De Keyser, R.; Liu, S.; Ionescu, C.M. Nonlinear predictive control applied to steam/water loop in large scale ships. *IFAC-PapersOnLine* **2019**, *52*, 868–873. [CrossRef]